105 (2026) 106475

Contents lists available at ScienceDirect

Poultry Science

journal homepage: www.elsevier.com/locate/psj

Full-Length Article

Single-cell transcriptomics reveals diversity and conservation of chicken lymphocytes

Huichao Liu [a,b], Junhao Tu [a,b], Xi He [a,b], Qingyuan Ouyang [a,b], Haihan Zhang [a,b,*]

[a] College of Animal Science and Technology, Hunan Agricultural University, Changsha, Hunan 410128, China
[b] Yuelu Mountain Laboratory, Changsha, Hunan 410128, China

ARTICLE INFO

Keywords:
Chicken immunology
Single-Cell RNA sequencing
Lymphocytes
Potential sex dimorphism
Cross-Species conservation

ABSTRACT

The domestic chicken (Gallus gallus) is a critical model for immunology and a major agricultural species, yet a comprehensive single-cell census of its immune architecture is lacking. Here, we constructed a high-resolution single-cell transcriptome atlas of three primary immune organs (thymus, bursa of Fabricius, and spleen) from chickens. Our analysis identified 24 distinct immune and stromal cell types, mapping their organ-specific distributions: B cells were predominantly localized to the bursa of Fabricius, while T cell subsets were enriched in the thymus. We delineated developmental trajectories and identified key transcription factors governing lineage commitment, including TCF12 for $CD4^+CD8^+$ T cells and SOX13 for T helper 2 cells. Further analysis revealed potential sexually dimorphic immune maturation, where B cells exhibited sex-biased gene expression primarily in early differentiation stages, whereas T cell differences were most pronounced during proliferation. Cross-species comparison demonstrated remarkable conservation of core immunoregulatory circuits, with transcription factors like MEF2C, LEF1, and GATA3 playing conserved roles in avian and mammalian immunity. This resource provides a foundational framework for understanding avian immune defense, advancing poultry disease-resistant breeding, and offers evolutionary insights into vertebrate immunology.

Introduction

As the most economically important poultry species, the immune function of chickens directly determines their resistance to major infectious diseases such as avian influenza and Newcastle disease, and crucial for the development of poultry industry (Koutsakos et al., 2019; Sun et al., 2023; Taylor et al., 2016). Furthermore, the chicken serves as a core model animal for studying immune evolution in vertebrates (Brown et al., 2003). In contrast to the human immune system, chickens exhibit both evolutionary conservation and species-specific characteristics, offering a unique perspective for deciphering vertebrate immune functions and validating human immune-related mechanisms (Mallaby et al., 2022). The principal immune organs for the chicken including the thymus, bursa of Fabricius, and spleen, are essential for mounting immune responses and mediating vaccine efficacy. The thymus and bursa of Fabricius function as primary lymphoid organs, responsible for receiving immune signals and producing immune cells, whereas the spleen acts as a secondary lymphoid organ, facilitating immune cell activation and proliferation (Ceccopieri and Madej, 2024; Seto, 1981; Yang and Liu, 2023). Although B- or T-lineage cells in chickens have been previously identified through the expression of specific surface markers or transcriptional factors (Burkhardt et al., 2022; Ko et al., 2018), traditional bulk RNA sequencing lacks the resolution to reveal immune cell subtype heterogeneity. This limitation hinders the ability to capture fine-grained intercellular functional differences or to reconstruct dynamic regulatory processes during immune responses (Dai et al., 2023; Kolodziejczyk et al., 2015; Tu et al., 2025).

In recent years, breakthroughs in single-cell RNA sequencing (scRNA-seq) technology have provided a powerful tool for resolving cellular heterogeneity in complex organs. This technology has enabled precise definition of cell subtypes and in-depth exploration of functional mechanisms in human and mouse immune system research (Wang et al., 2023; Winkels et al., 2018). However, in chickens, existing studies mostly focus on specific immune cell types within individual tissues (Dai et al., 2023; Liu et al., 2023; Maxwell et al., 2024; Shah et al., 2021; Zhang et al., 2025). A systematic single-cell atlas that integrates multiple immune organs is still lacking. Consequently, the core and conserved transcriptional regulators governing immune cell identity, as well as the developmental and maturation trajectories of immune cell lineages across different tissues in chickens, remain largely unexplored.

* Corresponding author at: College of Animal Science and Technology, Hunan Agricultural University, Changsha, Hunan 410128, China.
E-mail address: zhhous@163.com (H. Zhang).

https://doi.org/10.1016/j.psj.2026.106475
Received 21 November 2025; Accepted 17 January 2026
Available online 18 January 2026

To address these limitations, we collected three primary immune organs (thymus, bursa of Fabricius, and spleen) from both male and female chickens and performed single-cell RNA sequencing to construct a comprehensive panoramic atlas of the avian immune system. After quality control, we obtained a total of 72,627 cells and identified 24 distinct cell types. These were annotated using both classical and chicken-specific marker genes, such as *XCL1* and *IL2RB*, which we found to be specifically expressed in chicken Natural Killer T (NK T) cells. Furthermore, our study explored sex-biased gene expression across immune cell types and delineated immune cell populations and genetic mechanisms conserved with humans. This work provides novel insights into the cellular basis of chicken immunity and simultaneously offers valuable cross-species evidence for understanding vertebrate immune evolution and human immune-related diseases.

Materials and methods

Tissue collection and ethics statement

In this study, thymus, spleen, and bursa of Fabricius samples were collected from three 90-day- old yellow-feathered chickens (two female and one male). The detailed sample information is provided in Supplementary Table 1. All chickens were raised under the same feeding and environmental conditions until the day of sampling. All animal experiments were approved by the Animal Ethics Committee of Hunan Agricultural University (Permit No. 202100269).

Cell suspension for scRNA-seq

After washing with 1× Dulbecco's Phosphate Buffered Saline (DPBS), tissue samples were enzymatically digested for 25 min using an enzyme mixture (2.5 ml RPMI + collagenase IV, 2 mg/ml). The reaction was terminated by adding 3× volume of RPMI-1640 complete medium. Digested samples were filtered through a 70 μm cell strainer, then centrifuged at 350×g for 5 min at 4°C. The cell pellet was resuspended and diluted with Wash Buffer (1× DPBS with 0.04 % BSA and 0.01 mM EDTA) based on total cell count. After re-filtration through a 40 μm cell strainer, the cell suspension was stained with trypan blue and analyzed via a Bio-Rad TC20 cell counter. Qualified suspensions (target concentration: 700 – 1200 cells/μl) were used for on-machine labeling (Supplementary Table 1).

Library construction and sequencing

Single-cell suspensions were quality-checked with Countess® II (0.4 % trypan blue, 9:1 ratio), ensuring ≥90 % viability and ≥1000 cells/μL. For 10X Genomics isolation, cell-enzyme mixtures were combined with barcode gel beads and encapsulated into Gel Bead-In-Emulsions (GEMs) via microfluidic system. After lysis, barcoded cDNA was synthesized by reverse transcription, followed by PCR post-emulsion breaking. cDNA fragments (200 - 300 bp) underwent library construction with adapter ligation (P5, R1) and PCR. Libraries were quantified by Qubit 3.0, qualified via Agilent 2100, then sequenced on Illumina NovaSeq 6000 (PE150) with paired-end mode: Read1 (16 bp barcode, 10 bp UMI) for cell identification/quantification, Read2 for genome alignment.

scRNA-seq data analysis

Raw sequencing data were processed with CellRanger (v7.1.0) for quality control and alignment to the chicken GRCg7b genome. The R (v4.2.0) package Seurat (v4.3.0) was used to create the CreateSeuratObject (min.cells = 3, min.features = 200), and 2000 variable features were identified via FindVariableFeatures (selection.method = "vst"). Low-quality cells (abnormal nFeature_RNA or high percent.mt) were filtered with ddqcR (v0.1.0), and doublets removed using DoubletFinder (v2.0.3) (detailed QC criteria in Supplementary Table 2). Batch effects were corrected with Harmony (v0.1.1). Using top 30 PCs, FindNeighbors constructed cell relationships, and clustree (v0.5.0) determined optimal resolution (0.2) for FindClusters. Cluster markers were identified with FindAllMarkers (only.pos = TRUE, min.pct = 0.25, logfc.threshold = 0.25), and cell types were annotated via CellMarker 2.0 and literatures. Based on the expression of classic marker genes for G2/M and S phases, the score of each cell's potential cell cycle stage was calculated. The CellCycleScoring function was used to compute the cell cycle score for each cell, and the calculated scores for S phase and G2/M phase were stored in the metadata.

Transcription factor analysis

Orthologous genes between chicken (GRCg7b) and human (GRCh38) were first identified using biomaRt (v2.54.1) in R (v4.2.0) via the getLDS function, retaining one-to-one orthologs with gene symbols and Ensembl IDs. Cross-cell-type transcription factor (TF) analysis was done in Python (v3.9) with pySCENIC (v0.12.1), including inferring TF-target interactions via grn, prioritizing targets through Cistarget motif enrichment (10 kb TSS-flanking regions, GRCh38), and computing per-cell TF activity scores with AUCell for cross-cell type comparisons. A minimum of 10 genes was required for a regulon to be retained, and regulons with too few target genes were filtered out. Additionally, the Regulon Specificity Score (RSS) was used to quantify the enrichment level of each regulon in distinct cell types. Note that this analysis relied on human-chicken orthologs and human genome-based motif enrichment, which may miss chicken-specific regulatory elements or TF-binding differences.

Cell-cell communication analysis

Cell-cell communication was analyzed in R (v4.2.0) using CellChat (v1.6.1). A CellChat object was constructed using createCellChat with CellChatDB.human, with "Secreted Signaling" subsets filtered via subsetDB. The full gene set was included via subsetData; overexpressed ligand-receptor genes/interactions were identified, and data projected onto the human PPI network (PPI.human) using projectData. Communication probabilities were calculated with computeCommunProb (raw.use = TRUE), and pairs with <10 cells filtered via filterCommunication. This analysis assumed conservation of ligand-receptor interactions and PPIs between humans and chickens; potential avian-specific differences should be considered when interpreting results.

Inference of differentiation trajectory

Inferring cellular lineage trajectories using Monocle3 (v1.3.4). We constructed differentiation trajectories for chicken T cells and B cells under UMAP dimensionality reduction. During trajectory and pseudotime computation, naive T cells and naive B cells were treated as root states, respectively.

Identification and comparison of sex-differentially expressed genes

Differential expression analysis between male and female groups was performed based on the normalized gene expression matrix. Sex-differentially expressed genes (sex-DEGs) were identified using three methods: edgeR (v3.40.2) (Robinson et al., 2010), MAST (v1.24.1) (Finak et al., 2015), and Seurat FindMarkers function (incorporating the MAST algorithm) (Hao et al., 2021). The filtering criteria were as follows: for edgeR, FDR < 0.05 and $|\log_2 FC| > 1$; for MAST, p_value < 0.05 and $|\log_2 FC| > 0.5$; and for FindMarkers, adj.p < 0.05 and $|\log_2 FC| > 0.5$ (MAST and FindMarkers have almost no genes available for analysis when log2FC>1, so we relaxed the conditions). Functional enrichment analyses (KEGG and GO) of the sex-DEGs were conducted using clusterProfiler (v4.6.2). UpSetR (v1.4.0) was used to generate intersection

matrix plots, which visualize the overlapping relationships of sex-DEGs among different cell subtypes.

Cross-species analysis

Single-cell transcriptomic data of human thymus were obtained from the E-MTAB-8581 dataset (Park et al., 2020) (the SRA numbers are SRR26592232, SRR26592233, SRR26592234), containing 23,603 cells from 13- and 24-year-old adolescent samples. The same preprocessing pipeline was used as the chicken dataset, with 19,418 cells retained post-quality control. Shared homologous genes between the two datasets served as anchors for batch effect correction via FindIntegrationAnchors. From normalized data, the top 1,000 highly variable genes were selected to calculate inter-cell-type Spearman correlation coefficients. Human transcription factors were retrieved from AnimalTFDB v4.0 (Shen et al., 2022); cell type-specific DEGs were intersected with this list to obtain conserved transcription factors between chickens and humans.

Results

Landscape of single-cell atlas across chicken primary immune organs

We analyzed and integrated single-cell transcriptomic data from the cells collected from the thymus, spleen, and bursa of Fabricius in chickens (Fig. 1A). After stringent quality control to remove low-quality cells and potential doublets, a total of 72,627 cells were retained for downstream analysis, with a median of 5,067 expressed genes and 51,266 sequencing reads per cell (Supplementary Table 2). Following batch effect correction and unsupervised clustering (Supplementary Figure S1A-C), we identified 24 transcriptionally distinct cell clusters (Fig. 1B, Supplementary Table 3). These clusters were categorized into 10 cell type groups: B cell, classic dendritic cells, epithelial cells, erythrocyte, fibroblast, macrophage, plasma cells, plasmacytoid dendritic cells, platelet, and T cells (Figure S1D).

The 24 annotated cell types were meticulously defined using established and novel maker genes: T cell lineages included naive T cells (*CD3D, CCR7*), naive $CD4^+$ T cells (*CD3D, CD4*), naive $CD8^+$ T cells (*CD3D, CDA8*), $CD4^+CD8^+$ T cells (*CD4, CD8A*), activated $CD4^+$ T cells (*ICOS, CD4*), activated $CD8^+$ T cells (*ICOS, CD8A*), proliferative $CD8^+$ T cells (*ICOS, CD8A, TOP2A*), T helper 2 cells (*CD3D, GATA3*), $CD4^+$ T helper 2 cells (*CD3D, GATA3 CD4*), proliferative T helper 2 cells (*TOP2A, PCNA, CD3D, GATA3*), NK T cell (*GNLY, XCL1, IL2RB*), and proliferative T cells (*TOP2A, PCNA, CD3D*). B cell lineages comprised B cell (*CD79B, PAX5*), pre-B cells (*VPREB3, EBF1*), plasma cells (*MZB1, JCHAIN*). Innate immune and stromal populations included macrophage (*CD74, C1Q1*), classical dendritic cells (*NAAA, CXCL13*), plasmacytoid dendritic cells (*NAAA, INFAR1*), platelets (*TUBB1, ITGB3*), erythrocytes (*HBBA, HBA1*), fibroblasts (*COL1A1, COL3A1*), and epithelial cells (*EPCAM, SPINK5*). Visualization of marker gene expression confirmed that cells within the T cell group specifically expressed not only classic pan-T cell markers like CD3D and CD3E but also the non-classical regulator BCL11B (Fig. 1C). Similarly, the B cell group was characterized by high expression of canonical marker genes *EBF1* and *PAX5* (Anand et al., 2021; He et al., 2021) (Fig. 1C). Furthermore, we discovered that *CD44* exhibited broad expression across all immune-related cell types but was largely absent in non-immune cells, such as erythrocytes, platelets, fibroblasts, and epithelial cells, suggesting its utility for distinguishing these cell types (Fig. 1C).

Analysis of cell type composition across the three immune organs revealed distinct and specialized enrichment of specific cell types, aligning with their known physiological functions (Fig. 1D). The bursa of Fabricius was overwhelmingly dominated by B cell lineages, which constituted 91.24 % of its cellular population. Within this group, proliferative B cells (50.29 %), Pre-B cells (20.06 %), and mature B cells (20.55 %) represented the major subsets. Conversely, the thymus was predominantly composed of T cells, accounting for 83.16 % of its cells, with $CD4^+CD8^+$ double-positive T cells alone making up the largest fraction (36.22 %), reflecting its role as the primary site for T cell development. The spleen, as a secondary lymphoid organ, contained a mixed population supportive of its role in systemic immune responses, with substantial proportions of both T cells (71.11 %) and B cells (20.84 %). We further identified tissue-specific cell types, defined as those with over 90 % of their total population residing in a single organ (Figure S1E). This analysis confirmed $CD4^+$ T helper 2 cells, proliferative T helper 2 cells, and proliferative T cells as thymus-dominant. Pre B cells were uniquely bursa of Fabricius-dominant, while NK T cells and plasmacytoid dendritic cells were identified as spleen-dominant populations.

Furthermore, we investigated the proliferative dynamics and sexual dimorphism of the immune landscape. Cell cycle phase analysis confirmed that nominally proliferative cell types, including proliferative $CD8^+$ T cells, proliferative T helper 2 cells, proliferative T cells, and proliferative pre-B cells, exhibited a characteristically higher proportion of cells in the S phase compared to their non-proliferating cell types (Fig. 1E). Screening for potential sex-differentially expressed genes (sDEGs) across all cell types revealed a total of 2,361 sDEGs, the majority of which were mapped to B cell and T cell lineages. Notably, we did not detect any sDEGs in Proliferative $CD8^+$ T cells, a result likely attributable to their limited cell numbers and the high transcriptional heterogeneity inherent to their actively cycling state, which may obscure consistent sex-based differences.

Transcriptional regulation and intercellular communication network across chicken immune cell types

Building on the cellular landscape of chicken immune organs, we focused on T and B lymphocytes to delineate their subtypes and developmental trajectories, clarifying how immune cells differentiate into functional lineages. To delineate the regulatory programs governing cell identity, we compared cell type-specific transcriptional regulons across all 24 populations. This analysis identified key transcription factors specifically associated with distinct immune lineages, including *TCF12* for $CD4^+CD8^+$ T cells, E2F1 for proliferative pre-B cells, *SOX13* and *GATA3* for T helper 2 cells, *EZH2* for NK T cells, and *XRCC4* for broad T cell populations (Supplementary Figure S2A). Correlation analysis of the top regulons revealed that cells with related functions or developmental potentials shared similar regulatory networks. For instance, naive $CD4^+$ T cells and naive $CD8^+$ T cells exhibited closely alighed regulon patterns involving factors like ONECUT2, ASCL2, and EOMES, while mature B cell showed a regulatory profile comparable to their precursor, proliferative pre-B cells (Fig. 2A). A global assessment of transcriptional similarity further supported these relationships, showing that proliferative cell types such as Proliferative pre-B cells, pre B cells, Proliferative $CD8^+$ T cells, and proliferative T cells, clustered together, whereas terminally differentiated plasma cells formed a distinct group (Fig. 2B).

Given that immune cells coordinate responses through intricate communication networks, we next leveraged our single-cell data to infer intercellular crosstalk by analyzing ligand-receptor co-expression. We constructed a comprehensive cell-cell communication profile, which revealed frequent and complex singaling interactions both within and between different immune cell types (Fig. 2C). Our analysis indicated that the proliferating cell types (such as pre-B cells, proliferative B cells, proliferative $CD8^+$ T cells) were generally prominent signal senders, while more terminally differentiated or specialized cells (such as mature B cells, plasmacytoid dendritic cells, macrophages, activated $CD8^+$ T cells) primarily acted as signal receivers (Fig. 3D). Summarizing the outgoing signals identified the BAFF and MK pathways as exclusively enriched in the B cell group, while the MIF pathway was predominantly active within the T cell group (Fig. 3E). Further dissection showed that the BAFF pathway functioned predominantly in an autocrine manner within the B cell compartment, whereas the MK pathway mediated

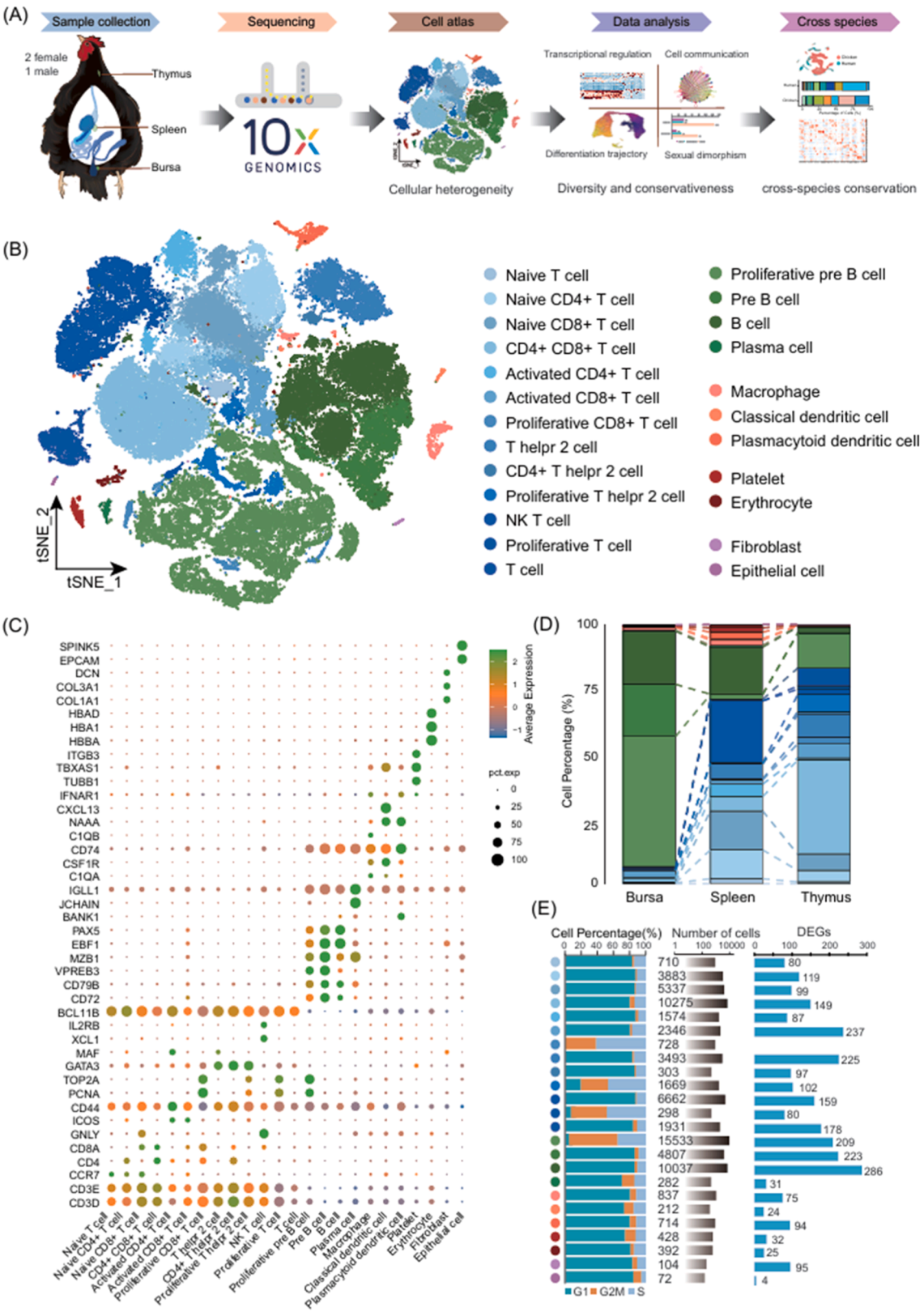

Fig. 1. Landscape of the single-cell atlas of three chicken immune organs.
(A) Workflow of this study. (B) The single-cell atlas landscape merged with three immune organs, thymus, spleen, and bursa. Each major cell lineage is used as the similar color scale. (C) Bubble plot of marker genes annotated for 24 cell types. The size of the dots represents the expression ratio of genes in the corresponding cell type, while color difference represents the average expression level of genes. (D Stacked bar chart displaying the proportion of each cell type in the thymus, bursa, and spleen of chickens. The same cell types in different organs are connected by dashed lines. (E) The cell proportion in different cell stages (left), cell numbers (middle), and sex-differential expressed gene numbers (right) among 24 cell types.

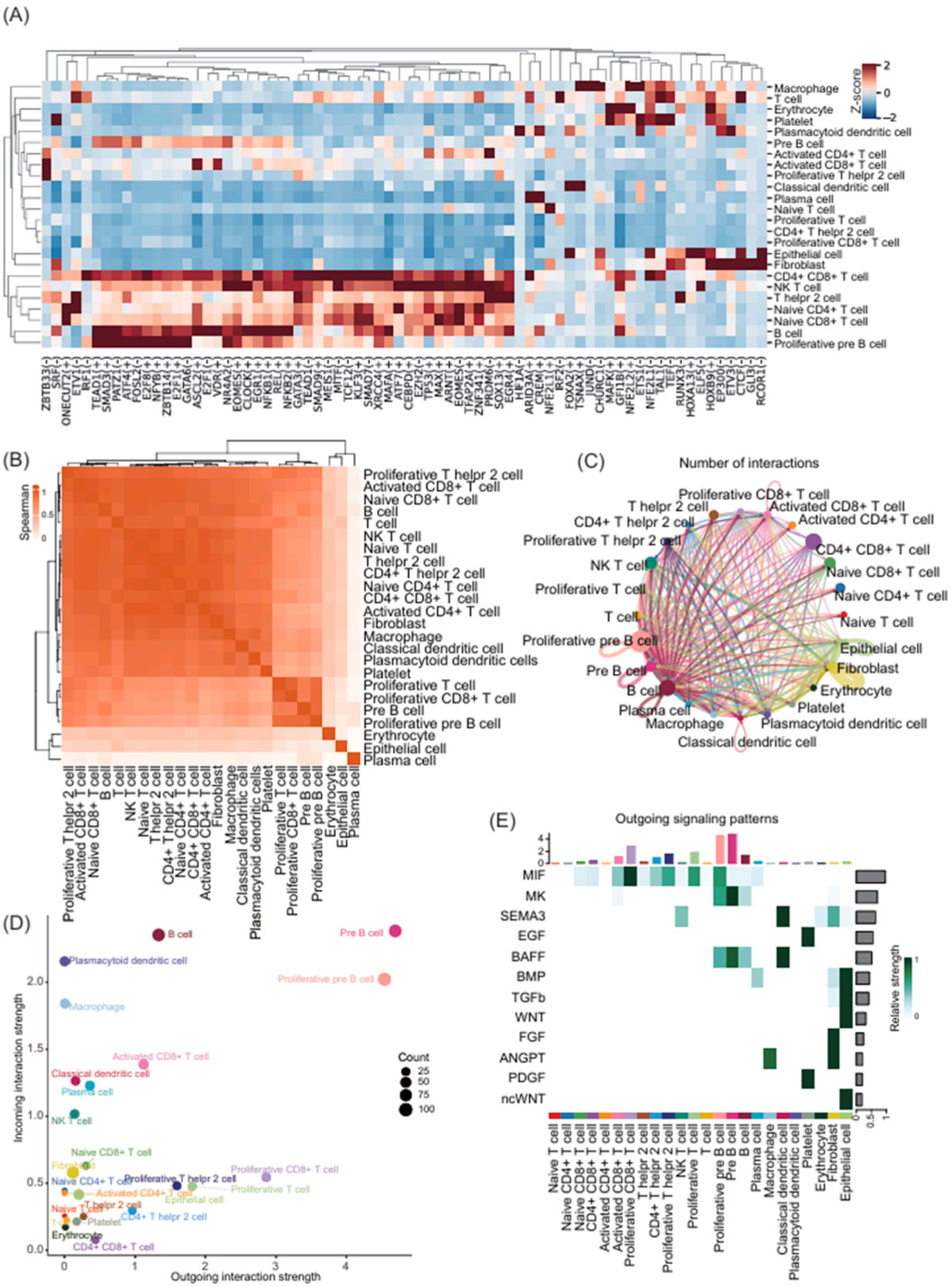

Fig. 2. Transcriptional regulation and intercellular communications across chicken immune cells.
(A) Heatmap of the top 5 cell type-specific transcription factors in each cell type. The color represents the standardized value of the regulon specificity score. (B) Spearman correlation analysis of expression profiles between different cell types using the top 1000 highly variable genes. (C) Cell-cell communication network diagram between different cell types analyzed by CellChat. The thickness of the line represents the number of communications. (D) Scatter plot showing the input and output strength of communication signals between different cell types. (E) Pattern heatmap of communication signaling pathways between different cell types.

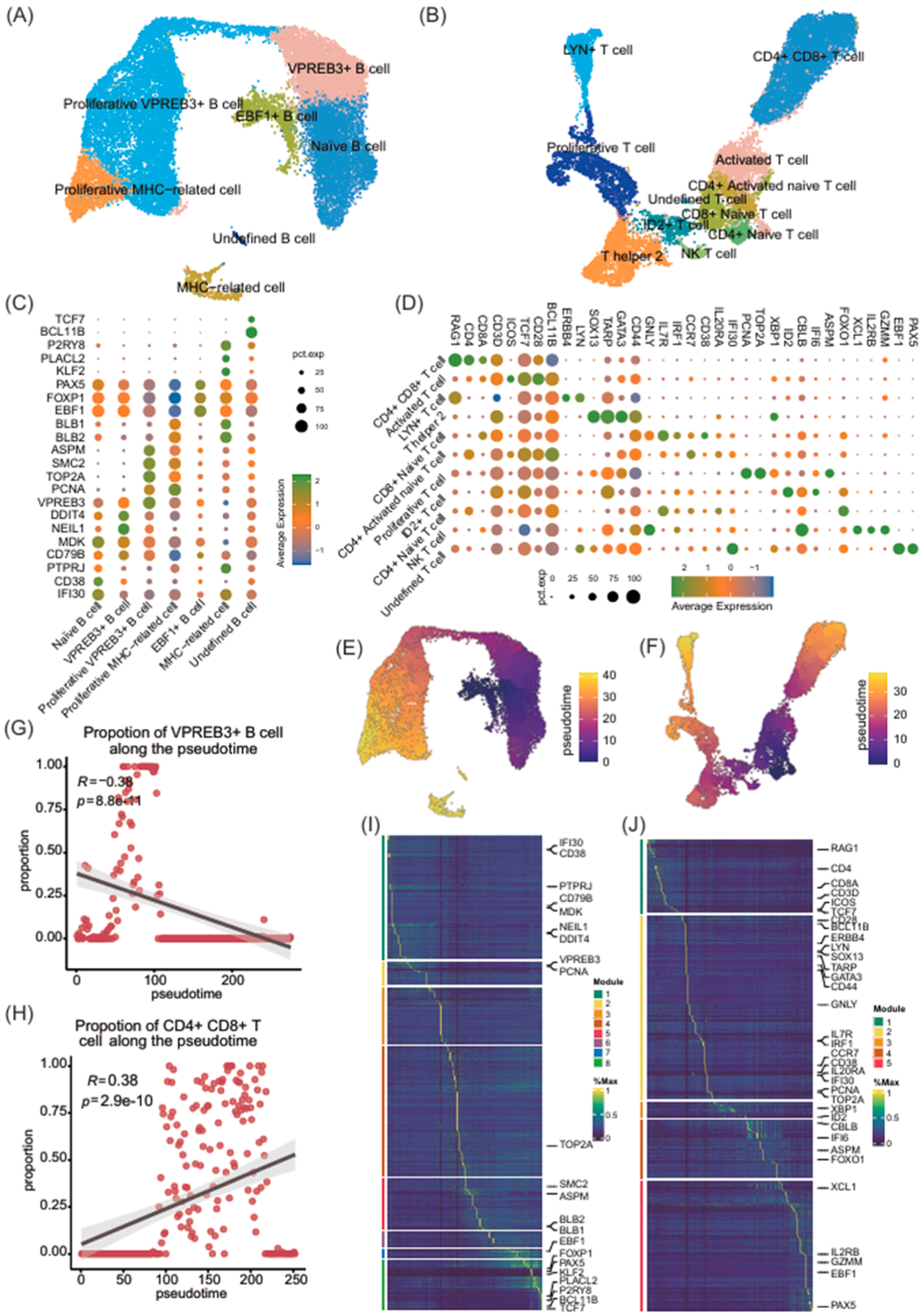

Fig. 3. Analysis of lymphocyte heterogeneity and developmental trajectories in chicken immune cells.
(A) 7 cell subtypes identified in B cells from bursa. (B) 11 cell subtypes identified in T cells from thymus. (C) Bubble plot of marker genes for B cells. (D) Bubble plot of marker genes for T cell subtypes. (E) Pseudotime trajectory analysis of B cells in the bursa. (F) Pseudotime trajectory analysis of T cells. (G) The change of VPREB$^+$ B cell proportion with pseudotime progress. (H) The change of CD4$^+$CD8$^+$ T cell proportion with pseudotime progress. (I) Module enrichment analysis of pseudotime-dependent differentially expressed genes (q value < 0.001) in B cells. (J) Module enrichment analysis of pseudotime-dependent differentially expressed genes (q value < 0.001) in T cells.

communication from B cells to other cell types (Supplementary Figure S2B). Interestingly, the MIF pathway represented a specific channel of communication from T cells to B cells, suggesting a potential role for T cells in antigen presentation to B cells (Klasen et al., 2014) (Supplementary Figure S2C). We further classified the relationships of cell communication into 5 patterns and found the similar results that T cell group and B cell group were enriched with their cell-specific pathways (Supplementary Figure S3A and B).

Heterogeneous cell subtype and developmental cell trajectory of chicken lymphocytes

To elucidate the molecular mechanisms of lymphocyte identity and differentiation, we analyzed cell-type-specific transcriptional regulatory networks and intercellular communication pathways underlying immune system function. As the principal mediators of humoral immunity, responsible for pathogen presentation and antibody production respectively, T and B cells are central to adaptive immune defense (Ritzau-Jost and Hutloff, 2021). To deeply characterize their heterogeneity and development, we aggregated T cells from the thymus and B cells from the bursa of Fabricius for sub-clustering and trajectory analysis. This high-resolution approach defined 6 distinct subtypes within the B cell lineage, including naive B cell (*CD38, IFI30*), EBF1$^+$ B cells (*EBF1, PAX5, FOXP1*), VPREB3$^+$ B cells (*VPREB3, PAX5*), proliferative VPREB3$^+$ B cells (*TOP2A, SMC2, VPREB3, PAX5*), proliferative MHC-related cells and MHC-related cells (*BLB1, BLB2, PAX5*), and one undefined cell type (Fig. 3A and C).

Similarly, we identified 11 subtypes within the T cell lineage, including CD4$^+$ CD8$^+$ T cells (*CD3, CD4, CD8A*), activated T cells (*CD3, ICOS, CD28*), LYN$^+$ T cells (*LYN, RAG1, ERBB4*), T helper 2 cells (*CD3D, GATA3*), CD8$^+$ naive T cells (*CD8A, CCR7*), CD4$^+$ activated naive T cells (*CD4, ICOS, CCR7*), proliferative T cells (*TOP2A,PCNA,CD3D*), ID2$^+$ T cells (*TARP, ID2, IFI6*), CD4$^+$ naive T cells (*CD4, CCR7*), NK T cells (*CD3D, GNLY, XCL1,GZMM*), and one undefined T cells (Fig. 3B and D).

Constructing the developmental trajectories revealed a clear progression for both lineages. B cell development originated from naive B cells and culminated in the terminally differentiated MHC-related cells (Fig. 3E). In contrast, T cell development branched early from CD4$^+$ and CD8$^+$ naive T cells into two major pathways: one leading to CD4$^+$CD8$^+$ T cells and the other to LYN$^+$ T cells (Fig. 3F). Furthermore, the shifting cell type composition along the pseudotime axis validated these trajectories (Fig. 3G and 3H, Supplementary S3A-E). For example, the proportions of proliferative subtypes (such as VPREB3$^+$ B cells) (Ekman et al., 2012) decreased over time (Fig. 3G). However, the fractions of functional, effector-like subtypes (such as MHC-related B cells and CD4$^+$CD8$^+$ T cells) (Zhu et al., 2023) increased (Fig. 3H).

Analysis of dynamic gene expression further elucidated the underlying molecular programs. During B cell development, proliferation-related genes like *VPREB3, PCNA*, and *TOP2A* were highly expressed in early and middle stages, while antigen-presentation genes *BLB1* and *BLB2* dominated the late stage (Fig. 3I). In the T cell lineage, genes involved in T cell receptor rearrangement, such as *RAG1* (Brauer et al., 2016), were characteristic of the early stage, whereas the expression of effector molecules like *XCL1* marked the late, functionally mature stage of differentiation (Fig. 3J).

Potential sex-differential gene expression and pathways in B and T lymphocytes

Sexual dimorphism in avian species is strongly influenced by transcriptional differences in Z-chromosome genes, largely due to the absence of global dosage compensation in birds (Papanicolaou et al., 2025). However, the landscape of sex-based gene expression differences at cellular resolution remains largely unexplored. To address this, we systematically identified sDEGs in B and T lymphocytes using three distinct statistical methods: MAST, Seurat's FindMarkers, and edgeR. A comparative analysis revealed that edgeR was the most sensitive method, identifying 125 sDEGs in B cells and 76 in T cells, compared to fewer sDEGs identified by MAST (36 in B, 14 in T) and FindMarkers (34 in B, 28 in T) (Fig. 4A). A robust core set of sDEGs was confirmed by the intersection of all three methods, yielding 27 high-confidence sDEGs in B cells and 8 in T cells (Fig. 4B and C).

To understand the functional implications of these sex differences, we performed KEGG pathway enrichment analysis on the sDEGs identified by edgeR. This exploratory analysis identified potential cell-type-specific pathways: sDEGs in B cells were significantly enriched for Protein processing in endoplasmic reticulum, Terpenoid backbone biosynthesis, and the MAPK signaling pathway, driven by key genes like *HSP90AA1* and *HSPA8* (Fig. 4D). In T cells, sDEGs were enriched in the Spliceosome, Ribosome, and Protein processing in endoplasmic reticulum pathways (Fig. 4E). Even though the same MAPK signaling pathway was enriched for both B and T cells sDEGs, the genes involved in this pathway were distinct, with *MEF2C* and *FOS* in B cells but *HSPA2* and *STMN1* in T cells, suggesting the sex alters the cell-type specific changes of gene expression involved in different signaling pathways.

Further investigation into the distribution of sDEGs across B and T cell subtypes revealed that the majority were specific to individual cell types (Fig. 4F and G). However, a small fraction of sDEGs was shared across nearly all subtypes; these were predominantly located on the Z chromosome (Supplementary Figure S4), underscoring the broad, cell-type-agnostic impact of sex-chromosome dosage. Strikingly, the temporal concentration of sex-biased expression also differed between lineages: in the B cell lineage, sDEGs were concentrated in early differentiation stages (e.g., VPREB3$^+$ B cells, naive B cells), whereas in the T cell lineage, they were most prominent during active proliferation (e.g., Proliferative T cells).

Cross-species analysis of thymus scRNAseq data between chicken and human

With the cellular and molecular features of the chicken immune system established, we performed an integrated comparative analysis of single-cell transcriptomic data from chicken thymus and a public human thymus dataset to evaluate the evolutionary conservation of lymphocyte biology. The human data were processed through an identical quality control pipeline, resulting in 19,418 high-quality cells for integration with our chicken data. Manual annotation based on canonical marker gene expression identified 16 distinct, homologous cell types common to both species (Fig. 5A, B and D). Despite this conserved cellular taxonomy, the relative abundance of these cell types was disproportionately distributed between the species (Fig. 5B). The human thymus was enriched for proliferating T cells, T helper 17 cells, and memory T cells, whereas the chicken thymus contained significantly greater proportions of naive T cells and CD4$^+$CD8$^+$ double-positive T cells (Fig. 5C).

We next quantified transcriptomic similarity by calculating gene expression correlations. As expected, correlations between cell types within a species (average $r = 0.71$) were substantially higher than correlations for the same cell type across species (average $r = 0.41$) when using the top 2,000 highly variable genes (Fig. 5E). This indicates that species-specific expression patterns dominate the most variable transcriptome features. However, when the analysis was expanded to include all homologous genes, several key immune cell types, including macrophages ($r = 0.56$), proliferating cells ($r = 0.67$), and CD8$^+$ T cells ($r = 0.58$), demonstrated significant conservation between chickens and humans (Supplementary Figure S5).

Strikingly, the expression of key transcriptional regulators was robustly conserved across the evolutionary divide. We identified a core set of transcription factors with conserved cell-type-specific expression patterns, including *MEF2C* and *BCL11A* in B cells, *HMGB3* in proliferating cells, *LEF1* in CD8$^+$ T cells, *GATA3* in T helper 2 cells, and *STAT3* in regulatory T cells (Tregs) (Fig. 5F). This conservation implies that the fundamental regulatory circuitry governing lymphoid cell fate and

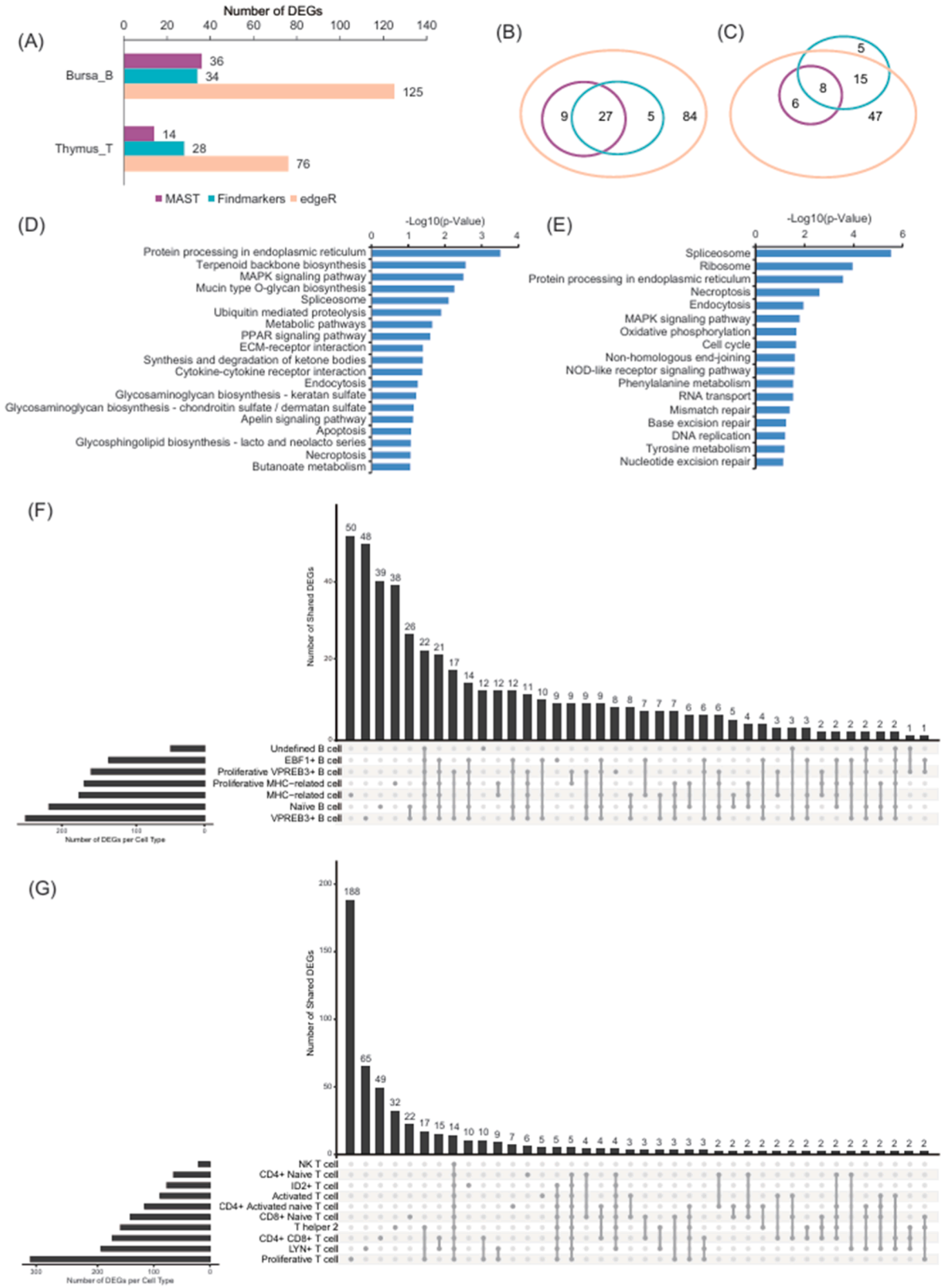

Fig. 4. Sex-differential expressed genesand pathway enrichment in B and T lymphocytes.
(A) Bar chart showing the number of sex-differential expressed genes (sDEGs) in B cells and T cells identified by three different methods (MAST, Findmarkers, EdgeR). (B) Venn diagram of sDEGs in B cells identified by different methods; (C) Venn diagram of sDEGs in T cells identified by different methods. The different colors represent different methods. (D) KEGG pathway enrichment analysis of sDEGs in B cells (E) KEGG pathway enrichment analysis of sDEGs in T cells. F-G) Upset table of shared sDEGs for B (F) and T (G) cell subtypes, respectively.

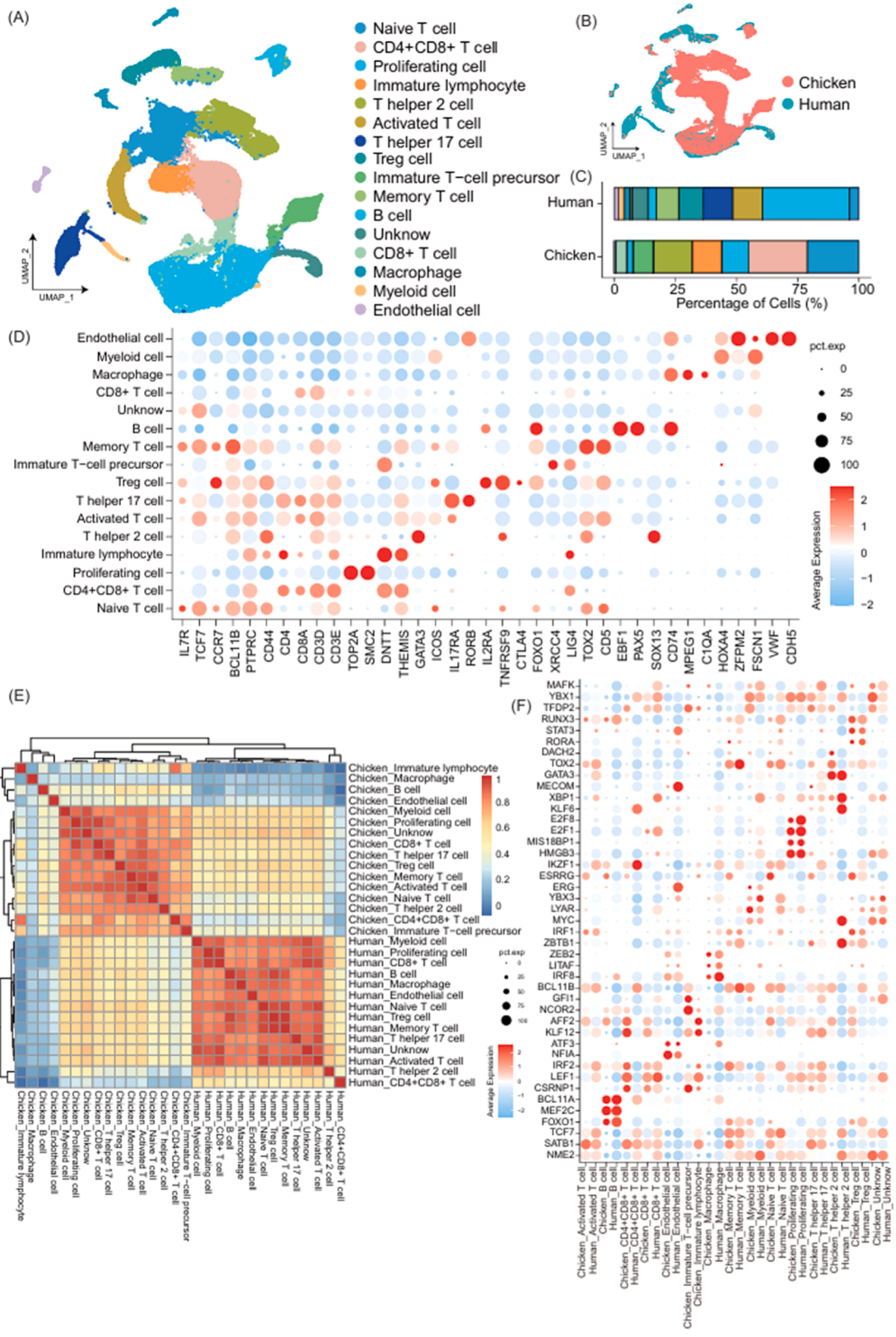

Fig. 5. Cross-species comparative analysis of the thymus single-cell transcriptome between human and chicken.
(A) Single cell atlas of thymus between human and chicken. (B) The distribution of cells originated from chicken and human. (C) Bar chart showing the cell proportion composition in chicken and human thymus. (D) Bubble plot of marker genes used for cell type annotated in chicken and human thymus. (E) Heatmap to show the transcriptomic similarity of cell types between chicken and human thymus using the top 1000 highly variable genes. (F) Comparison of the gene expression of key transcription factors across cell types in chicken and human thymus.

function has been maintained for the evolution between avian and mammalian species.

Discussion

Our study provides a comprehensive single-cell atlas of the chicken immune system by integrating transcriptomic data from three primary immune organs: the thymus, bursa of Fabricius, and spleen. We identified 24 distinct cell types and systematically characterized their molecular features, transcriptional regulation, developmental trajectories, and evolutionary conservation. This work addresses critical gaps in avian immunology and offers valuable insights for both basic research and agricultural applications. Specifically, our multi-dimensional analysis bridges avian and mammalian immunology, refining current principles of vertebrate immune system organization while highlighting species-specific adaptations that shape poultry immune function.

Cellular composition and tissue specialization

Unlike previous studies focused on single tissues, our multi-tissue approach reveals the systemic organization of chicken immunity. The bursa of Fabricius was dominated by B cell lineages (91.24 %), particularly proliferative B cells and pre-B cells, confirming its role as the primary site for B cell development (Berghof et al., 2019). In early B cell development, *VPREB3* plays a non-redundant role in enabling pre-BCR-mediated survival and differentiation signals (Ekman et al., 2012; Nguyen et al., 2021). The thymus contained predominantly T cells (83.16 %), with $CD4^+CD8^+$ double-positive T cells representing the largest subset (36.22 %), while the spleen showed a mixed population supporting its function as a peripheral immune organ. We identified several novel cell types, including MHC-related B cells expressing avian-specific *BLB1* and *BLB2* genes localized to the chicken MHC-B region (Kaufman, 2022; Zhang et al., 2020) and LYN^+ T cells characterized by low *CD3D* expression (Ozgür et al., 2008; Sanal et al., 1996), suggesting specialized functional states in avian immunity.

Conserved transcriptional regulation

Our analysis revealed remarkable conservation of transcriptional regulatory networks between chickens and mammals. We identified key transcription factors with cell-type-specific expression patterns, including *TCF12* for $CD4^+CD8^+$ T cells, which aligns with its known role in regulating Th cell differentiation in humans (Emmanuel et al., 2018; Mesman and Smidt, 2017); *SOX13* and *GATA3* for T helper 2 cells, with *GATA3* being a well-recognized key regulator of Th2 cell differentiation in mammals (Kumagai et al., 2024), and E2F1 for proliferative pre-B cells, consistent with the role of the mammalian E2F family in regulating B cell proliferation and differentiation (Fang et al., 2022; Zou et al., 2015).The co-enrichment of *SOX13* and *GATA3* in chicken Th2 cells implies potential cooperation in maintaining Th2 cell function (In et al., 2017; Spidale et al., 2018). These conserved transcriptional circuits highlight an evolutionarily stable regulatory core that emerged early in vertebrate evolution, ensuring the robustness of T and B cell lineage commitment across species. The retention of these TF modules in chickens—despite the unique tissue niche of bursa-dependent B cell development—suggests that core immune regulatory logic is decoupled from species-specific developmental contexts, providing a mechanistic basis for using chicken models to study universal vertebrate immune processes.

Notably, our cell-cell communication analysis revealed a discrepancy in signaling profiles between proliferative pre-B cells and Th2 cells. Pre-B cells clustered with general proliferative cells, while Th2 cells showed a distinct signature. This reflects their divergent functions: pre-B cell proliferation is developmentally programmed to expand precursor pools, aligning with core proliferative cell signaling. In contrast, Th2 cell proliferation is antigen-induced and geared toward immune effector function, with signaling dominated by regulatory cues rather than proliferation drivers. This highlights that proliferative immune cell communication profiles are shaped by both proliferation state and functional orientation.

Developmental trajectories and lineage commitment

Pseudotime analysis revealed distinct differentiation pathways for B and T lymphocytes that match the known functional division of the thymus and bursa of Fabricius as central immune organs (Funk and Palmer, 2003; Zúñiga-Pflücker, 2004). B cell development in the bursa of Fabricius progressed from naive B cells through $VPREB3^+$ stages to terminal MHC-related cells, while T cell development in the thymus branched from $CD4^+$ and $CD8^+$ naive T cells into $CD4^+CD8^+$ T cells and LYN^+ T cell lineages. The identification of MHC-related cells and LYN^+ T cells as terminal differentiation states suggests these populations represent functionally specialized endpoints, with MHC-related cells potentially functioning as antigen-presenting B cells and LYN^+ T cells exhibiting unique functional modes in immune defense or regulation (Parker and Kaufman, 2017; Sun et al., 2021).

Potential sexual dimorphism in immune function

Our analysis revealed that sex-differential genes in B cells are concentrated in early differentiation stages and enriched in endoplasmic reticulum protein processing pathways involving *HSP90AA1* and *HSPA8*, while in T cells they are prominent during proliferation stages and involved in spliceosome functions. The MAPK signaling pathway plays a central role in regulating sex differences in both lineages, consistent with findings in other species (Nicoll et al., 2018; Sheppard et al., 2021; Sultana et al., 2023), but utilizes distinct genes, such as *MEF2C* and *FOS* in B cells versus *HSPA2* and *STMN1* in T cells. These stage-specific effects mirror observations in mammals where sex hormones impact B cell maturation and T cell function (Staerk et al., 2025).

For poultry production, these sex-differential immune patterns may underpin observed differences in disease susceptibility and feed conversion efficiency between male and female chickens—key economic traits. For example, the enrichment of endoplasmic reticulum protein processing pathways in female B cells could enhance antibody production capacity, while spliceosome-related sex differences in T cells may modulate immune response dynamics. Future validation with larger cohorts could enable targeted breeding strategies to improve flock immunity and productivity.

Evolutionary conservation and species specificity

Comparative analysis revealed thymus lymphobiology features of conserved core plus species-specific specialization, strongly supporting chickens as an immunological research model (Tregaskes and Kaufman, 2021). Chickens showed higher proportions of naive T cells and $CD4^+CD8^+$ T cells, potentially an adaptation for defending airborne pathogens (Chen et al., 2025), while humans contained more proliferative T cells, Th17 cells and memory T cells, matching complex immune demands (Wakahara et al., 2012). Key transcription factors including *MEF2C* and *BCL11A* in B cells, *HMGB3* in proliferative cells, *LEF1* in $CD8^+$ T cells, *GATA3* in Th2 cells and *STAT3* in Tregs showed conserved expression patterns, forming an evolutionarily retained immune regulatory core that enables using chicken models to study conserved immune mechanisms.

Notably, our cross-species analysis uncovered a key clustering pattern (Fig. 5E): cells grouped primarily by species when using the top 2,000 highly variable genes, whereas the same cell types across species exhibited higher similarity when using all homologous genes. This discrepancy arises because highly variable genes are enriched for species-specific adaptive traits, while homologous genes capture the evolutionarily conserved core programs that define cell identity. This

observation highlights that species-specific divergence is concentrated in adaptive gene sets, whereas the fundamental molecular signatures of immune cell types are retained across vertebrates.

Limitations of the study

While this study provides a comprehensive single-cell atlas of the chicken immune system, two main limitations should be noted. First, technical and analytical constraints exist: a uniform enzymatic digestion protocol across distinct immune organs may cause mild cell-type recovery bias; our transcriptional regulatory and cell-cell communication analyses relied on human-chicken orthologs and conserved molecular network assumptions, which could overlook avian-specific features, and these computational inferences lack experimental validation. Second, the exploratory analysis of potential sexual dimorphism was constrained by a small, unbalanced sample size (2 female, 1 male), limiting the robustness of related conclusions. Corresponding future optimizations include: adopting tissue-specific digestion protocols; integrating chicken-specific regulatory resources and validating key molecular interactions experimentally (e.g., ChIP-seq for TF binding, co-culture assays for ligand-receptor pairs); and expanding sample sizes with balanced sex ratios to verify potential sexual dimorphism.

Conclusions

This study establishes the first comprehensive single-cell atlas of the chicken immune system, revealing a core cellular and regulatory architecture conserved with mammals alongside crucial avian specializations. We defined 24 cell types across three organs, identified deeply conserved transcriptional regulators like *GATA3* and *E2F1* governing lymphocyte identity, and uncovered lineage-specific sexual dimorphism where B and T cells exhibit distinct sex-biased gene expression patterns at different developmental stages. These findings not only provide the molecular foundation for advancing disease-resistant poultry breeding but also solidify the chicken's role as a powerful model for decoding fundamental principles of vertebrate immune evolution.

Data availability

The single-cell RNA sequencing (scRNA-seq) raw data, processed expression matrices, and metadata generated in this study have been deposited in the Genome Sequence Archive (GSA) at the China National Center for Bioinformation (CNCB) with the accession number CRA030201, which is publicly available. For further assistance or access-related questions, please contact the corresponding author H.H.Z. (zhhous@163.com).

Funding

This study was funded by grants from the Yuelu Mountain Laboratory Seed Industry Project (YLS-2025-2Y 04050), the China Agriculture Research System (CARS-41) and Hunan Agriculture Research System (HARS-06).

CRediT authorship contribution statement

Huichao Liu: Writing – original draft, Visualization, Investigation, Formal analysis. **Junhao Tu:** Visualization, Methodology. **Xi He:** Project administration, Funding acquisition, Data curation. **Qingyuan Ouyang:** Supervision, Methodology. **Haihan Zhang:** Writing – review & editing, Methodology, Funding acquisition.

Disclosures

The authors declare that there is no conflict of interest.

Acknowledgements

We sincerely thank Hunan Xiangjia Animal Husbandry Co., Ltd. for providing the experimental animals and technical support throughout this study.

Supplementary materials

Supplementary material associated with this article can be found, in the online version, at doi:10.1016/j.psj.2026.106475.

References

Anand, P., Guillaumet-Adkins, A., Dimitrova, V., et al., 2021. Single-cell RNA-seq reveals developmental plasticity with coexisting oncogenic states and immune evasion programs in ETP-ALL. Blood 137 (18), 2463–2480.
Berghof, T.V.L., Matthijs, M.G.R., Arts, J.A.J., et al., 2019. Selective breeding for high natural antibody level increases resistance to avian pathogenic Escherichia coli (APEC) in chickens. Dev. Comp. Immunol. 93, 45–57.
Brauer, P.M., Pessach, I.M., Clarke, E., et al., 2016. Modeling altered T-cell development with induced pluripotent stem cells from patients with RAG1-dependent immune deficiencies. Blood 128 (6), 783–793.
Brown, W.R., Hubbard, S.J., Tickle, C., et al., 2003. The chicken as a model for large-scale analysis of vertebrate gene function. Nat. Rev. Genet. 4 (2), 87–98.
Burkhardt, N.B., Elleder, D., Schusser, B., et al., 2022. The discovery of chicken Foxp3 demands redefinition of avian regulatory T cells. J. Immunol. 208 (5), 1128–1138.
Ceccopieri, C., Madej, JP., 2024. Chicken secondary lymphoid tissues-structure and relevance in immunological research. Animals (Basel) 14 (16).
Chen, Z.-Y., Gao, F.-Z., Bai, H., et al., 2025. Airborne free DNA in chicken farms: The overlooked traits in microbial diversity, viral composition, and antimicrobial resistance risk. J. Hazard. Mater. 499, 140144.
Dai, M., Zhu, S., An, Z., et al., 2023. Dissection of key factors correlating with H5N1 avian influenza virus driven inflammatory lung injury of chicken identified by single-cell analysis. PLoS Pathog. 19 (10), e1011685.
Ekman, A., Ilves, M., Iivanainen, A., 2012. B lymphopoiesis is characterized by pre-B cell marker gene expression in fetal cattle and declines in adults. Dev. Comp. Immunol. 37 (1), 39–49.
Emmanuel, A.O., Arnovitz, S., Haghi, L., et al., 2018. TCF-1 and HEB cooperate to establish the epigenetic and transcription profiles of CD4(+)CD8(+) thymocytes. Nat. Immunol. 19 (12), 1366–1378.
Fang, Z., Lin, M., Chen, S., et al., 2022. E2F1 promotes cell cycle progression by stabilizing spindle fiber in colorectal cancer cells. Cell Mol. Biol. Lett. 27 (1), 90.
Finak, G., Mcdavid, A., Yajima, M., et al., 2015. MAST: a flexible statistical framework for assessing transcriptional changes and characterizing heterogeneity in single-cell RNA sequencing data. Genome Biol. 16, 278.
Funk, P.E., Palmer, JL., 2003. Dynamic control of B lymphocyte development in the bursa of fabricius. Archivum immunologiae et therapiae experimentalis 51 (6), 389–398.
Hao, Y., Hao, S., Andersen-Nissen, E., et al., 2021. Integrated analysis of multimodal single-cell data. Cell 184 (13), 3573-3587.e3529.
He, X., Smith, S.E., Chen, S., et al., 2021. Tumor-initiating stem cell shapes its microenvironment into an immunosuppressive barrier and pro-tumorigenic niche. Cell Rep. 36 (10), 109674.
In, T.S.H., Trotman-Grant, A., Fahl, S., et al., 2017. HEB is required for the specification of fetal IL-17-producing γδ T cells. Nat. Commun. 8 (1), 2004.
Kaufman, J., 2022. Innate immune genes of the chicken MHC and related regions. Immunogenetics 74 (1), 167–177.
Klasen, C., Ohl, K., Sternkopf, M., et al., 2014. MIF promotes B cell chemotaxis through the receptors CXCR4 and CD74 and ZAP-70 signaling. J. Immunol. 192 (11), 5273–5284.
Ko, K.H., Lee, I.K., Kim, G., et al., 2018. Changes in bursal B cells in chicken during embryonic development and early life after hatching. Sci. Rep. 8 (1), 16905.
Kolodziejczyk, A.A., Kim, J.K., Svensson, V., et al., 2015. The technology and biology of single-cell RNA sequencing. Mol. Cell 58 (4), 610–620.
Koutsakos, M., Kedzierska, K., Subbarao, K., 2019. Immune Responses to Avian Influenza Viruses. J. Immunol. 202 (2), 382–391.
Kumagai, T., Iwata, A., Furuya, H., et al., 2024. A distal enhancer of GATA3 regulates Th2 differentiation and allergic inflammation. Proc. Natl. Acad. Sci. U S A 121 (27), e2320727121.
Liu, W., Xu, Z., Qiu, Y., et al., 2023. Single-cell transcriptome atlas of newcastle disease virus in chickens both in vitro and in vivo. Microbiol. Spectr. 11 (3), e0512122.
Mallaby, J., Ng, J., Stewart, A., et al., 2022. Chickens, more than humans, focus the diversity of their immunoglobulin genes on the complementarity-determining region but utilise amino acids, indicative of a more cross-reactive antibody repertoire. Front. Immunol. 13, 837246.
Maxwell, M., Söderlund, R., Härtle, S., et al., 2024. Single-cell RNA-seq mapping of chicken peripheral blood leukocytes. BMC Genomics. 25 (1), 124.
Mesman, S., Smidt, MP., 2017. Tcf12 is involved in early cell-fate determination and subset specification of midbrain dopamine neurons. Front. Mol. Neurosci. 10, 353.
Nguyen, H.T.T., Guevarra, R.B., Magez, S., et al., 2021. Single-cell transcriptome profiling and the use of AID deficient mice reveal that B cell activation combined

with antibody class switch recombination and somatic hypermutation do not benefit the control of experimental trypanosomosis. PLoS Pathog. 17 (11), e1010026.
Nicoll, J., Fry, A., Mosier, E., 2018. Sex-based differences in resting MAPK, androgen, and glucocorticoid receptor phosphorylation in human skeletal muscle. Steroids 141.
Ozgür, T.T., Asal, G.T., Cetinkaya, D., et al., 2008. Hematopoietic stem cell transplantation in a CD3 gamma-deficient infant with inflammatory bowel disease. Pediatr. TransPlant 12 (8), 910–913.
Papanicolaou, N., Lentini, A., Wettersten, S., et al., 2025. Multi-layered dosage compensation of the avian Z chromosome by increased transcriptional burst frequency and elevated translational rates. Nat. Commun. 16 (1), 9088.
Park, J.E., Botting, R.A., Domínguez Conde, C., et al., 2020. A cell atlas of human thymic development defines T cell repertoire formation. Science 367 (6480).
Parker, A., Kaufman, J., 2017. What chickens might tell us about the MHC class II system. Curr. Opin. Immunol. 46, 23–29.
Ritzau-Jost, J., Hutloff, A., 2021. T Cell/B cell interactions in the establishment of protective immunity. Vaccines (Basel) 9 (10).
Robinson, M.D., Mccarthy, D.J., Smyth, GK., 2010. edgeR: a Bioconductor package for differential expression analysis of digital gene expression data. Bioinformatics 26 (1), 139–140.
Sanal, O., Yel, L., Ersoy, F., et al., 1996. Low expression of T-cell receptor-CD3 complex: a case with a clinical presentation resembling humoral immunodeficiency. Turk. J. Pediatr. 38 (1), 81–84.
Seto, F., 1981. Early development of the avian immune system. Poult. Sci. 60 (9), 1981–1995.
Shah, A.U., Li, Y., Ouyang, W., et al., 2021. From nasal to basal: single-cell sequencing of the bursa of Fabricius highlights the IBDV infection mechanism in chickens. Cell Biosci. 11 (1), 212.
Shen, W.-K, Chen, S.-Y., Gan, Z.-Q., et al., 2022. AnimalTFDB 4.0: a comprehensive animal transcription factor database updated with variation and expression annotations. Nucleic Acids Res. 51 (D1), D39–D45.
Sheppard P, Puri T, Galea L. 2021. Sex differences and estradiol effects in MAPK and Akt cell signaling across subregions of the hippocampus.
Spidale, N.A., Sylvia, K., Narayan, K., et al., 2018. Interleukin-17-producing γδ T cells originate from SOX13(+) progenitors that are independent of γδTCR signaling. Immunity. 49 (5), 857-872.e855.
Staerk, J., Conde, D.A., Tidière, M., et al., 2025. Sexual selection drives sex difference in adult life expectancy across mammals and birds. Sci. Adv. 11 (40) eady8433.
Sultana, Z., Dorel, M., Klinger, B., et al., 2023. Modeling unveils sex differences of signaling networks in mouse embryonic stem cells. Mol. Syst. Biol. 19 (11), e11510.
Sun, H., Li, H., Tong, Q., et al., 2023. Airborne transmission of human-isolated avian H3N8 influenza virus between ferrets. Cell 186 (19), 4074-4084.e4011.
Sun, Y., Yang, Y., Zhao, Y., et al., 2021. The role of the tyrosine kinase Lyn in allergy and cancer. Mol. Immunol. 131, 121–126.
Taylor Jr., R.L., Medarova, Z., Briles, W.E., 2016. Immune effects of chicken non-MHC alloantigens. Poult. Sci. 95 (2), 447–457.
Tregaskes, C.A., Kaufman, J., 2021. Chickens as a simple system for scientific discovery: the example of the MHC. Mol. Immunol. 135, 12–20.
Tu, J.H., Liu, B.G., Lin, B.J., et al., 2025. Single-cell transcriptomic atlas of the chicken cecum reveals cellular responses and state shifts during Eimeria tenella infection. BMC Genomics. 26 (1), 141.
Wakahara, K., Baba, N., Van, V.Q., et al., 2012. Human basophils interact with memory T cells to augment Th17 responses. Blood 120 (24), 4761–4771.
Wang, Z., Wu, Z., Wang, H., et al., 2023. An immune cell atlas reveals the dynamics of human macrophage specification during prenatal development. Cell 186 (20), 4454-4471.e4419.
Winkels, H., Ehinger, E., Vassallo, M., et al., 2018. Atlas of the immune cell repertoire in mouse atherosclerosis defined by single-cell RNA-sequencing and mass cytometry. Circ. Res. 122 (12), 1675–1688.
Yang, W., Liu, X., Wang, X., 2023. The immune system of chicken and its response to H9N2 avian influenza virus. Vet. Q., 43 (1), 1–14.
Zhang, L., Li, X., Ma, L., et al., 2020. A newly recognized pairing mechanism of the α- and β-chains of the chicken peptide-MHC class II complex. J. Immunol. 204 (6), 1630–1640.
Zhang, Q., Wang, Q., Zheng, J., et al., 2025. Single-cell RNA sequencing of the spleen reveals differences in Salmonella typhimurium infection mechanisms between different chicken breeds. Poult. Sci. 104 (2), 104669.
Zhu, M.Z., Xu, H.M., Liang, Y.J., et al., 2023. Edible exosome-like nanoparticles from portulaca oleracea L mitigate DSS-induced colitis via facilitating double-positive CD4(+)CD8(+)T cells expansion. J. Nanobiotechnology. 21 (1), 309.
Zou, Z., Chen, J., Liu, A., et al., 2015. mTORC2 promotes cell survival through c-Myc-dependent up-regulation of E2F1. J. Cell Biol. 211 (1), 105–122.
Zúñiga-Pflücker, JC., 2004. T-cell development made simple. Nat. Rev. Immunol. 4 (1), 67–72.